J Mater Sci (2009) 44:6736–6740
DOI 10.1007/s10853-009-3603-8

MESOSTRUCTURED MATERIALS

Lewis and Brønsted acids in super-acid catalyst SO_4^{2-}/ZrO_2–SiO_2

Yan Wang · Jinghong Ma · Dong Liang · Meimei Zhou · Fuxiang Li · Ruifeng Li

Received: 11 November 2008 / Accepted: 14 May 2009 / Published online: 30 May 2009

Abstract Super-acid catalyst, SO_4^{2-}/ZrO_2–SiO_2, with high zirconium loading was synthesized and the nature of the surface acid was investigated by FT-IR of pyridine adsorption. With the increasing ZrO_2 content, the Lewis and Brønsted acid sites increased and reached the maximum when Zr/Si (molar ratio) = 1.3. The sample with Zr/Si = 1.3 showed the strongest IR adsorption band in the S=O stretching region (1,300–1,400 cm^{-1}). Pyrosulfate and monosulfate species existed on the surface of the catalysts and the acidic strength could be enhanced by induction effect of their S=O groups. And there were two kinds of Brønsted acid sites on the surface of the catalysts.

Introduction

In recent years, sulfated-zirconia has attracted much attention due to its high activity to isomerize alkanes at relatively low temperature. It has been first claimed as a super-acid [1] with strong acidic and redox properties. The relatively small surface of sulfated-zirconia limited its use as a catalyst for some reactions [2]. Using mesoporous silica as neutral support we can overcome this disadvantage. Meosporous silica containing sulfated-zirconia not only has considerable high surface areas, but also distinguished acid properties [3, 4]. It has become well established that the performance of a heterogeneous catalyst depends not only on the intrinsic catalytic activity of its components, but also on its texture and stability.

It is well-known that the catalytic properties of sulfated-zirconia depend strongly on its surface acidity. Researchers have paid many efforts to the super-acid materials and tried to disclose the nature and strength of their surface acidity. Literature [5] revealed a method, the super-acid catalysts, SO_4^{2-}/ZrO_2–SiO_2, with SBA-15 structure and different zirconium contents were synthesized and showed excellent performance in the *n*-pentane isomerization at 308 K. Kanougi et al. [6] suggested the identification of the strong acid sites to sulfates linked to Zr^{4+} cations of low coordination by DFT quantum chemical calculations. Thus, the acid properties of the super-acid materials are highly influenced by zirconium content. From the above presentations, the effect of acidic types and distribution on catalysis performance attracts lots of attention and needs further investigation.

In this study, in situ FT-IR with pyridine as probe molecule was employed to investigate the acidic properties of the catalysts SO_4^{2-}/ZrO_2–SiO_2 with different Zr/Si ratio. The origin of the acidic properties in the super-acid catalysts is investigated and discussed, and a reasonable surface structural model of the catalyst is suggested.

Experimental

Sample preparation

Super-acid catalyst, SO_4^{2-}/ZrO_2–SiO_2, was directly synthesized by using tetraethyl orthosilicate (TEOS) and zirconium

This article was originally presented in 6th International Mesoporous Materials Symposium (IMMS) on Sep 2008 in Namur.

Y. Wang · J. Ma · D. Liang · M. Zhou · F. Li · R. Li (✉)
Institute of Special Chemicals, Taiyuan University of Technology, Taiyuan 030024, China
e-mail: rfli@tyut.edu.cn

D. Liang
e-mail: ldpillar@263.net

nitrate ($Zr(NO_3)_4 \cdot 3H_2O$) as silicon source and zirconium source, respectively. CTAB and tri-block poly(ethylene oxide)–poly(propylene oxide)–poly(ethylene oxide) (P123, EO_{20}–PO_{70}–EO_{20}, Aldrich) were used as templates. The method of preparation was described in detail in Ref. [5]. The samples with different Zr/Si molar ratio in starting mixture are denoted as SZS-0.3, SZS-0.7, SZS-0.9, SZS-1.3, SZS-1.5, where the numbers correspond to the Zr/Si molar ratio.

The sample of SBA-15 was prepared for comparison according to literature [7]. SBA-15 sample was treated with 1.0 M aqueous H_2SO_4 for 1 h, in which the proportion of liquid and solid was 15 mL solution with 1 g SBA-15. Then the solid was filtered and dried at room temperature and calcined in air flow at 823 K for 6 h. The sulfation treatment followed exactly the same way as ZrO_2–SiO_2 was treated.

Structural characterization

XRD patterns were recorded by using a Rigaku D/max-2500 diffractometer (Cu target, 40 kV, 100 mA). N_2 adsorption–desorption isotherms were obtained at 77 K on a NOVA 1200e analyzer. Surface area was calculated by using BET equation and pore size distribution was calculated by the BJH method using the desorption branch. Prior to N_2 adsorption, the samples were previously evacuated for 3.5 h at 573 K. High-resolution transmission electron microscopy (HRTEM) was measured with JEM-2010 electron microscope operated at 200 kV. The samples were supported on a Cu film and a carbon grid.

In situ infrared spectroscopy

The nature and strength of acid sites on SO_4^{2-}/ZrO_2–SiO_2 samples were studied by adsorption of pyridine followed by infrared spectroscopy. The FT-IR spectra were recorded with SHIMADAZU FT-IR 8400 spectrophotometer with a resolution of 4.0 cm^{-1}. A self-supported wafer (about 8 mg/cm^2) of test samples was placed inside a quartz IR cell equipped with CaF_2 windows. Samples were pretreated under dynamic vacuum($<10^{-4}$ Torr) at 523 K for 1 h, after cooling to room temperature the cell and wafer background spectra were recorded. IR spectra of adsorbed pyridine on test samples were obtained following exposure of the wafer to excess pyridine vapor at room temperature for 0.5 h. Finally, excess of pyridine was desorbed by evacuating the test samples at the desired temperature (namely, 423 K, 523 K, and 623 K) for 0.5 h. The samples were cooled to room temperature, and then the spectra were recorded. The spectra of pyridine adsorption were obtained by absorbance-subtraction of the sample background spectrum.

Results and discussion

Textural investigation

Figure 1a shows the XRD patterns with the range of 0.7–5° of SO_4^{2-}/ZrO_2–SiO_2 samples. A small-angle XRD peak at $2\theta = 0.9°$ is clearly observed, which indicates that SZS has a long-range hexagonal ordering. With the Zr/Si molar ratio increasing, the intensity of the peak at $2\theta = 0.9°$ decreases but still can be observed, suggesting the gradually lowering of the long-range ordering. The characteristic wide-angle XRD peaks belonging to the pure tetragonal ZrO_2 structure can be observed in Fig. 1b, and the intensity of the peaks increases with the increase of the Zr/Si ratio.

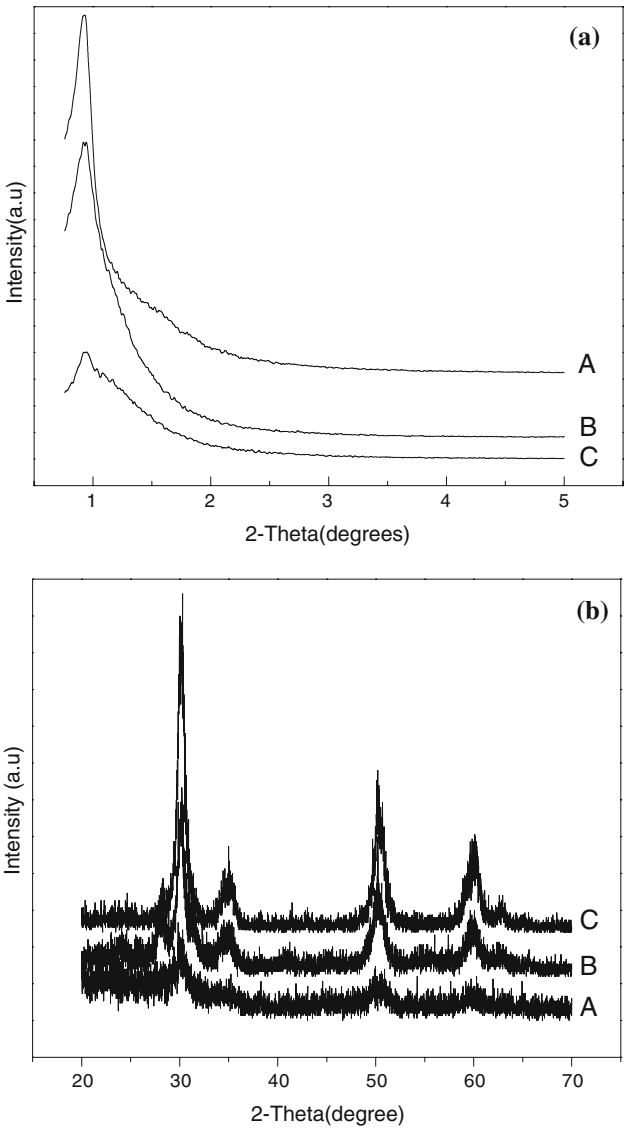

Fig. 1 XRD patterns of samples with different Zr/Si: A SZS-0.3, B SZS-1.3, C SZS-1.7

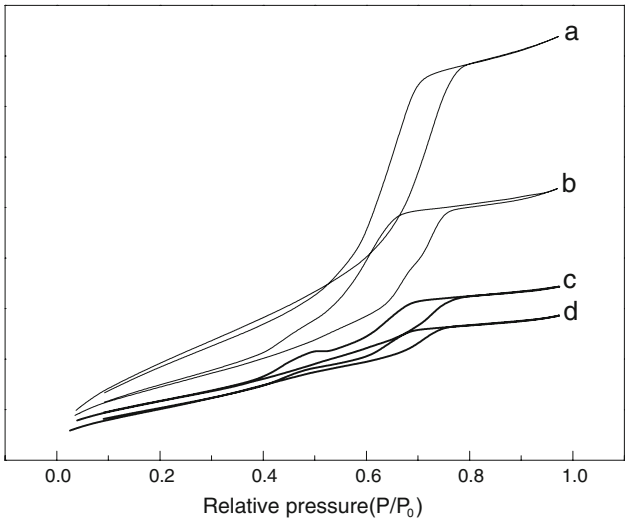

Fig. 2 N_2 adsorption–desorption isotherms of samples Zr/Si: (a) SZS-0.3; (b) SZS-0.7; (c) SZS-1.3; (d) SZS-1.7

Table 1 Pore structure parameters of samples

Samples	BET area (m^2/g)	Pore volume (cm^3/g)	Pore diameter (nm)	d_{100}	a_0	t (nm)
SZS-0.3	529.63	0.69	5.39	9.52	10.99	5.60
SZS-0.7	331.56	0.43	5.13	9.52	10.99	5.86
SZS-1.3	229.77	0.25	3.50	9.18	10.60	7.10
SZS-1.7	209.70	0.19	3.51	9.40	10.86	7.35

This result shows the single particle of ZrO_2 phase exists in the SO_4^{2-}/ZrO_2–SiO_2 samples.

The N_2 absorption–desorption isotherms and textural properties of SO_4^{2-}/ZrO_2–SiO_2 samples are given in Fig. 2 and Table 1, respectively. The isotherms of the samples are type-IV isotherms with a clear H_1 type hysteresis loops at high relative pressure, suggesting that the samples possess highly ordered framework with regular mesoporous channels. The mesopore diameter decreases from 5.39 to 3.51 nm with the increase of Zr/Si ratio. And the surface area of the samples varies from 529.63 (SZS-0.3) to 209.70 m^2/g (SZS-1.7).

Figure 3 shows the TEM images of the sample SZS-1.3. Well-ordered hexagonal arrays of mesopores with one dimension channels are observed, which indicates the hexagonal structure of SBA-15 has been retained. The SZS sample has thick channel walls with the average thickness ca. 4 nm.

In situ infrared spectra of pyridine adsorption

Figure 4 shows the in situ FT-IR spectra of desorption pyridine at 423 K on SZS0.3, SZS0.7, SZS0.9, SZS1.3, and

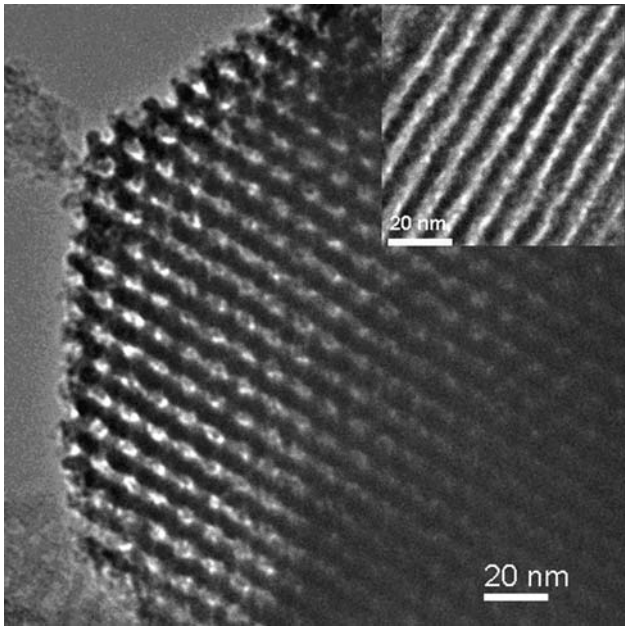

Fig. 3 TEM images of the sample SZS-1.3

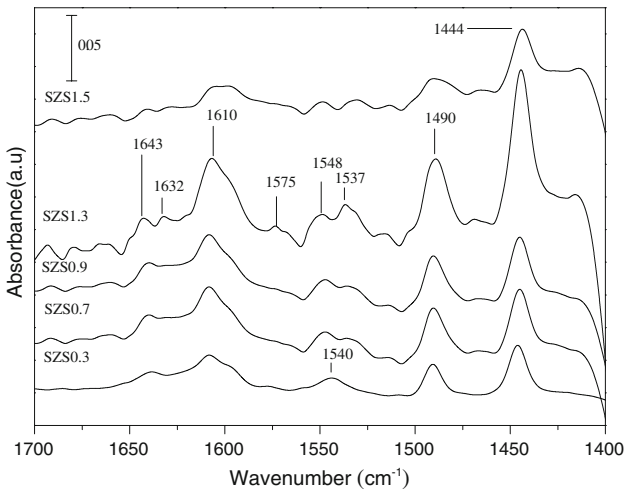

Fig. 4 In situ FT-IR spectra (νCNN region) of SO_4^{2-}/ZrO_2–SiO_2 with different Zr/Si ratio after pyridine adsorption at 423 K

SZS1.5 samples in the νCNN spectral region. Bands at 1,643, 1,610, 1,540, 1,490, and 1,444 cm^{-1} are registered on SZS0.3 sample. The 1,643 and 1,540 cm^{-1} bands are assigned to modes ν_{8a} and ν_{19b}, respectively, of pyridinium ion, and those at 1,610 and 1,444 cm^{-1} attributed to modes ν_{8a} and ν_{19b} of coordinated pyridine. With the Zr/Si ratio increasing, the band around 1,540 cm^{-1} apparently split into two bands 1,548 and 1,537 cm^{-1} and the shoulder peak at 1,632 cm^{-1} emerges clearly. This result implies the existence of at least two types of Brønsted acid sites on the surface of SO_4^{2-}/ZrO_2–SiO_2 samples. The integrated molar extinction coefficient is 1.67 cm/μmol for pyridine adsorbed on Brønsted sites in Si/Al based catalysts [8].

And using Beer' law, the surface concentration of Brønsted sites on the present materials is calculated as follows: SZS-0.3, 42.3 μmol/g; SZS-0.7, 87.5 μmol/g; SZS-0.9, 111.3 μmol/g; SZS-1.3, 157.0 μmol/g; SZS-1.5, 44.4 μmol/g.

Relative intensities of IR bands are continuously increasing along with the increasing Zr/Si molar ration until Zr/Si = 1.3. On SZS-1.5 sample (Fig. 4), bands at 1,643, 1,610, 1,537, 1,490, and 1,444 cm^{-1} still can be observed, but the intensities of those bands dramatically decrease. This result suggests that simply increasing zirconium content cannot always create more acid sites on surface of this $SO_4^{2-}/ZrO_2–SiO_2$ catalyst. To increase the acid concentration of catalysts, there are other factors we should beware of, such as the structural properties and the interaction between silica support and active components.

It should be noted that from silica support SBA-15, only two IR bands at 1,597 and 1,446 cm^{-1} attributed to ν_{8a} and ν_{19b} modes of hydrogen bonded pyridine, respectively, have been observed (Fig. 5). No band around 1,640, 1,540, and 1,490 cm^{-1} is observed in Fig. 5 indicating no new Lewis and Brønsted acid sites are created after sulfuric acid treatment of SBA-15. In other words, SBA-15 as pure silica supports its acidic property can not be affected by sulfuric acid treatment.

By incorporation of zirconium oxide, the surface acidity of the mesoporous silica has been changed. Not only new acid sites have been created but also the strength of the surface acid sites has been enhanced. And the concentration of surface acid on the SZS samples varies depending on the Zr/Si ratios. The SZS sample obtains the most acid concentration when Zr/Si = 1.3, and this result coincides with its catalytic performance in the *n*-pentane isomerization [5].

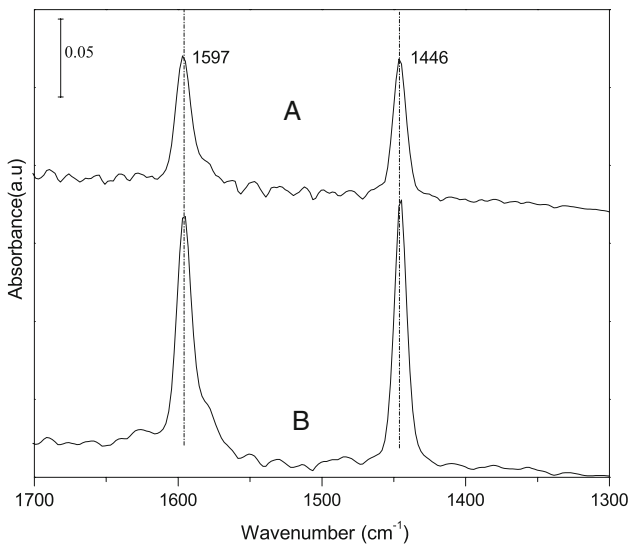

Fig. 5 In situ FT-IR spectra of SBA-15 (A) and sulfuric acid treated SBA-15 (B) after pyridine adsorption at 423 K

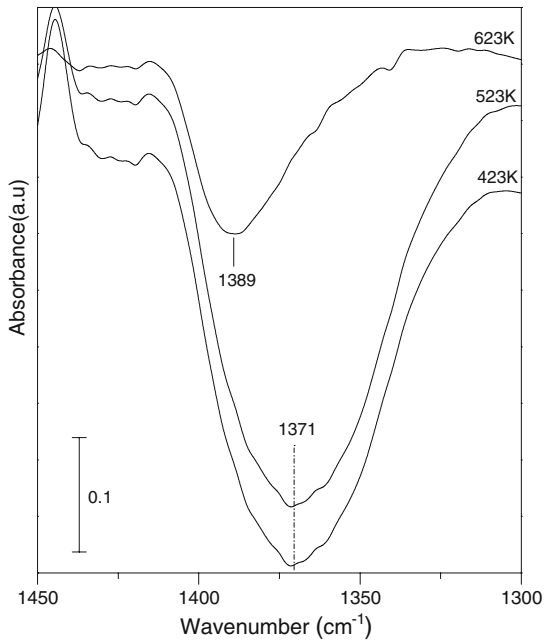

Fig. 6 In situ FT-IR spectra (sulfate region) of sample SZS-1.3 after pyridine adsorption at different temperatures

Figure 6 illustrates the absorbance in situ FT-IR spectra (sulfate region) of SZS-1.3 after pyridine adsorption relative to its background spectrum. In the S=O stretching region (1,340–1,440 cm^{-1}), SZS-1.3 sample shows strong negative IR adsorption band at 1,371 cm^{-1} at 423 K. The negative band of the S=O stretch can be attributed to an interaction between sulfate and pyridine resulting in a change to the double bond characteristics of S=O [9].

After increasing desorption temperature to 623 K, the intensity of this band decreases obviously and its minimum shifts upward to 1,389 cm^{-1}. This shift, together with the change of the intensity, suggests that the S=O stretching

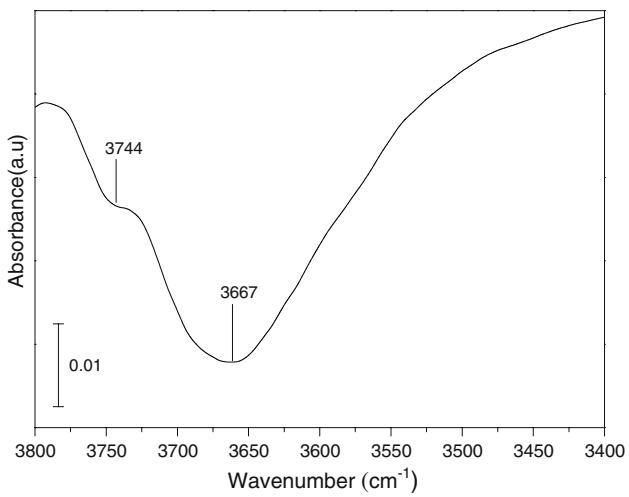

Fig. 7 FT-IR spectrum (hydroxyl region) of SZS-1.3 after pyridine adsorption at 423 K

Scheme 1 Proposed surface structural model and super-acid species

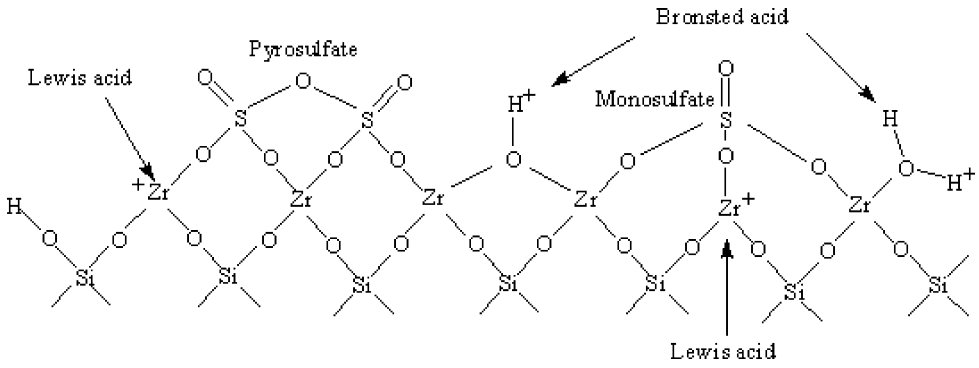

region has more than one component. According to several authors' descriptions [10, 11], two main sulfate species exist on the surface of sulfated-zirconia, pyrosulfate species with high frequency of the S=O stretching band at 1,405 cm^{-1} and monosulfate species with relatively low frequency at 1,380 cm^{-1}. And compared to our observation, the bands shift to low wavenumbers at 1,389 and 1371 cm^{-1}, respectively. Therefore, we suggest both pyrosulfate and monosulfate species exist on the surface of SZS samples. The shift of the S=O stretching band when increasing the desorption temperature to 623 K indicates the interaction between pyrosulfate species and pyridine is stronger than that between monosulfate species and pyridine. This result means pyrosulfate species provide stronger acid sites than monosulfate species.

In the OH stretching region (Fig. 7), SZS-1.3 show a main negative IR adsorption band at 3,667 cm^{-1} and a comparative weak band at 3,744 cm^{-1} after pyridine adsorption at 423 K. The 3,744 cm^{-1} band come from isolated Si–OH groups on SZS-1.3, while that at 3,667 cm^{-1} corresponds to the acidic bridged OH groups typical for sulfated-zirconia [12]. The formation of the negative bands is due to the interaction between pyridine and the OH groups. Basically, isolated Si–OH groups and bridged OH groups are recognized as hydrogen bond donor and Brønsted acid sites, respectively. The tail adsorption band next to 3,667 cm^{-1} at low frequency can be attributed to adsorbed H_2O next to a sulfate group [13]. Due to the strong inductive effects of S=O group, the adsorbed H_2O contributes as Brønsted acid center. The tail absorption band next to 3,667 cm^{-1} can also be due to heterogeneity of environment around the Brønsted sites [14].

Based on all the results and discussion above-mentioned, a logical surface structural model and the super-acid species are proposed (Scheme 1). The surface acid sites of the SZS samples are associated with the zirconium whose acidic strength can be strongly enhanced by induction effect of S=O groups.

Conclusions

Super-acid catalysts SO_4^{2-}/ZrO_2–SiO_2 with high Zr/Si ratio, high surface areas, and highly ordered mesoporosity have been synthesized. The catalysts have both Lewis and Brønsted acids and the surface acid sites are associated with Zr atoms. The concentration of the surface acid sites varies with the change of Zr/Si ratio, and reaches maximum when Zr/Si = 1.3. There are two types of sulfate species existing on the surface of the catalysts, pyrosulfate and monosulfate. And two kinds of Brønsted acid sites exist on the surface of the catalyst.

Acknowledgements Financial support of this work by the Natural Science Foundation of China (NSFC, No.50772070) is gratefully acknowledged.

References

1. Tanabe K, Yamaguchi T (1989) Stud Surf Sci Catal 44:99
2. Sun Y, Ma S, Du Y et al (2005) J Phys Chem B 109:2567
3. Akkari R, Ghorbel A, Essayem N, Figueras F (2007) Appl Catal A Gen 328:43
4. Akkari R, Ghorbel A, Essayem N et al (2008) Microporous Mesoporous Mater 111:62
5. Li F, Yu F, Li Y et al (2007) Microporous Mesoporous Mater 101:250
6. Kanougi T, Atoguchi T, Yao S (2002) J Mol Catal A 177:289
7. Zhao D, Feng J, Huo Q et al (1998) Science 279:548
8. Emeis CA (1993) J Catal 141:347
9. Jin T, Yamaguchi T, Tanabe K (1986) J Phys Chem 90:4794
10. Bensitel M, Saur O, Lavalley JC et al (1988) Mater Chem Phys 19:147
11. Morterra C, Cerrato G, Bolis V (1993) Catal Today 17:505
12. Steven RW Jr, Chuang SSC, Davis BH (2003) Appl Catal A Gen 252:57
13. Klose BS, Jentoft FC, Schlögl R (2005) J Catal 233:68
14. Tsyganemko AA, Storozheva EN, Manoilova OV et al (2000) Catal Lett 70:159